

Coulomb blockade in graphene quantum dots

Qiong Ma, Tao Tu,* Zhi-Rong Lin, Guang-Can Guo, and Guo-Ping Guo†

Key Laboratory of Quantum Information,

University of Science and Technology of China,

Chinese Academy of Sciences, Hefei, 230026, P.R.China

(Dated: October 17, 2018)

Abstract

We study the conductance spectrum of graphene quantum dots, both single and multiple cases. The single electron tunneling phenomenon is investigated and the periodicity, amplitude and line shape of the Coulomb blockade oscillations at low temperatures are obtained. Further, we discuss the transport behavior when multiple dots are assembled in array and find a phase transition of conductance spectra from individual Coulomb blockade to collective Coulomb blockade.

PACS numbers: 73.22.-f, 72.80.Rj, 73.21.La, 75.70.Ak

*Electronic address: tutao@ustc.edu.cn

†Electronic address: gpguo@ustc.edu.cn

Introduction. After first isolation from bulk graphite, graphene has attracted intense experimental and theoretical attention due to its unusual electronic spectrum and hence exotic properties [1, 2]. Moreover, its zero nuclear spin and weak spin-orbit interaction make it one of the most promising platforms for solid state quantum information processing. Design and fabrication of graphene quantum dot to confine Dirac fermion should be a critical step towards realizing such promise. There are alternative theoretical schemes proposed to deal with graphene's gapless spectrum and form quantum dot [3, 4, 5, 6]. Recently, single or double graphene quantum dots by etching nanoribbon into a charge island have been demonstrated [7, 8, 9, 10]. Although there are some initial studies [11, 12], the transport properties of graphene quantum dot are still remain to be explored both experimentally and theoretically.

In this paper, we study conductance of graphene quantum dots in both single dot and multiple dots regime, respectively. In previous theoretical studies, the conductance resonances are determined by the level of the (quasi-)bound states of the noninteracting electrons [3, 11, 12]. In the experiment the shape of the resonances will be governed by the electron interaction via the Coulomb blockade (CB) effect [7, 8, 9]. We use the Constant Interaction (CI) model to account for the intradot Coulomb interaction and perform an exact numerical calculation of the low bias conductance within quantum transport formalism [13]. The obtained CB peaks provides a simple way to describe the rich phenomena of transport physics in a variety of graphene quantum dots. In particular, we find the interdot tunneling would lead to a phase transition from individual CB to collective CB in the conductance spectra through multiple graphene quantum dots.

Graphene quantum dot. We begin by considering the graphene quantum dot on electrostatically confined graphene nanoribbon with semiconducting armchair boundary [4]. The electron wave function in graphene is usually described as a four-component (iso)spinor $\Psi = (\Psi_A^{(K)}, \Psi_B^{(K)}, \Psi_A^{(K')}, \Psi_B^{(K')})$. Close to the Dirac point, i.e. on low energy scales, a weakly doped (or undoped) graphene can be described by two identical and decoupled Dirac Hamiltonian

$$H_K = v_F \sigma \cdot p + U(x, y), \quad (1)$$

$$H_{K'} = v_F \sigma^* \cdot p + U(x, y), \quad (2)$$

where the Fermi velocity $v_F \approx 10^6$ m/s, the momentum operator $p = -i\hbar(\partial_x, \partial_y)^T$, Pauli matrices $\sigma = (\sigma_x, \sigma_y)$, $\sigma^* = (\sigma_x, -\sigma_y)$, and $U(x, y) = U(y)$ stands for the potential of applied electric field along y direction. We solve the equation $H\Psi = E\Psi$ respectively in left barrier, middle dot and right barrier to calculate the bound state energy within the conduction band if $V_{barrier} > V_{gate}$. According to the semiconducting armchair boundary conditions, the quantized transverse momentum is given as

$$q_n = \frac{(n + 1/3)\pi}{W}, n = 0, \pm 1, \dots \quad (3)$$

where W is the width of the ribbon. Additionally, after matching the wave function at $y = 0$ and $y = L$ (L is the length of dot), we can obtain discrete energy levels because of

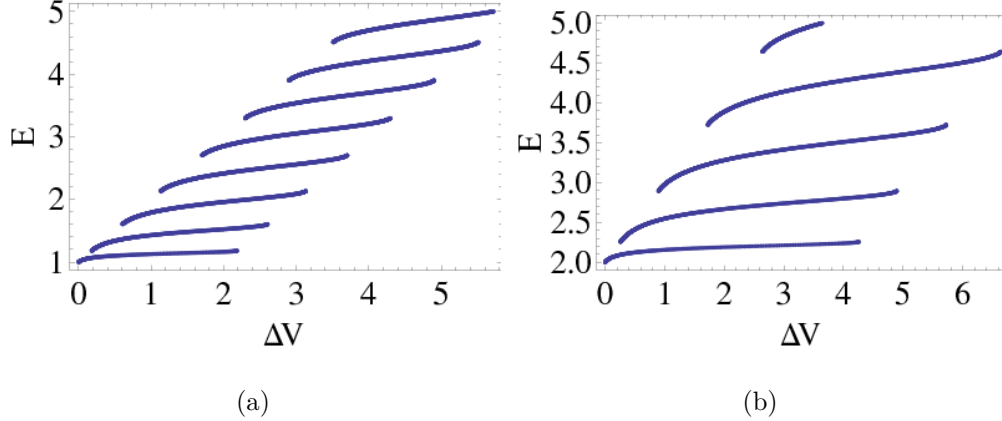


FIG. 1: Calculated energy levels in the graphene quantum dot for different quantized transverse momentum (a) q_0 , (b) q_{-1} . We consider a relatively long dot $q_0L = 5$ as in Ref. [4]. The horizontal axis stands for $\Delta V = V_{barrier} - V_{gate}$ and the vertical axis represents the electron bound energy, both in a unit of $\hbar v_F q_0$.

the electrostatical confinement in the longitudinal direction. The results are systematically shown in Fig. 1. The bound state energy levels only exist when E satisfies

$$E - eV_{gate} \geq \hbar v_F q_n \geq |E - eV_{barrier}|. \quad (4)$$

Coulomb blockade behavior. In the following analysis, we consider the five lowest quantized energy levels in the graphene quantum dot at potential barrier $\Delta V = 1$ in a unit of $\hbar v_F q_0$, of which three belong to q_0 , and two belong to q_{-1} . Here we set the nanoribbon width $W = 45$ nm according to Ref. [16], then $\hbar v_F q_0 = 0.015$ eV. First, we adopt the Constant Interaction (CI) model [13], which assumes that the Coulomb interaction between the electrons is independent of the number N of electrons in the dot and can be described by a constant capacitance C , and estimate the charging energy $e^2/C \approx 1$ in a unit of $\hbar v_F q_0$, which is constant for a given graphene quantum dot geometry and in the order of experimental measurements [7, 16]. In this model, the additional energy is $e^2/C + \Delta E$, where ΔE is the energy difference between two consecutive states. The CB peaks will appear if the gate charging can supplement the additional energy for next electron. Then we use the method described in Ref. [13] to discuss in detail the single electron tunneling phenomenon at low temperature in the weak tunneling regime ($\hbar\Gamma \ll k_B T \ll \Delta E$). The linear response conductance is

$$G = -\frac{e^2}{2k_B T} \sum_N \Gamma_N f'(E_N + U(N) - U(N-1) - E_F), \quad (5)$$

where $f(x) = \frac{1}{1+e^{\frac{x}{k_B T}}}$ is the Fermi-Dirac distribution function, E_N is the energy of the top filled single electron state for a N electron dot, $U(N) = (Ne^2)/2C - Ne\phi_{ext}$ in which $\phi_{ext} = \phi_0 + \alpha V_{gate}$, and E_F is the chemical potential of the lead. The width of localized

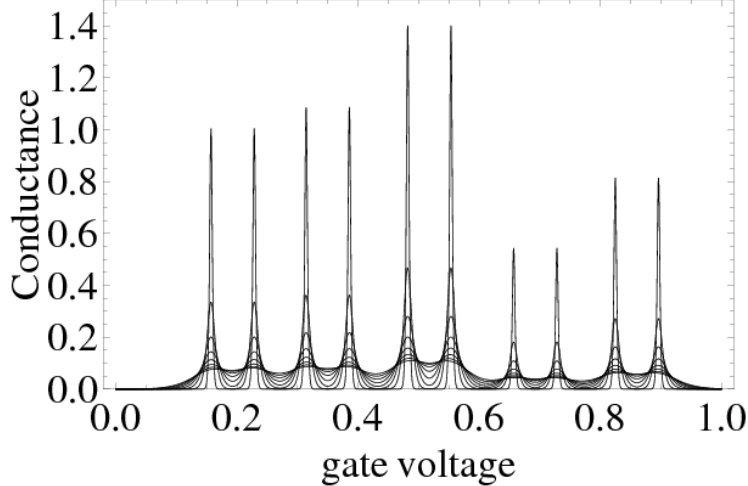


FIG. 2: Coulomb blockade oscillations for a graphene quantum dot at different temperatures. From top to bottom, $k_B T = 0.02, 0.06, 0.10, 0.14, 0.18, 0.22, 0.26, 0.30$, in a unit of $\hbar v_F q_0$. Spin freedom has been considered. The gate voltage is in a unit of eV and all the conductance peak heights are normalized by the first peak at $k_B T = 0.02$.

energy Γ in the above equation is determined by tunneling through the classically forbidden region [14]

$$T = \exp\left(-\int_L^{L+d} |k'| dy\right), \quad (6)$$

where $k' = i\sqrt{q_n^2 - ((E - eV_{\text{barrier}})/\hbar v_F)^2}$ is the vanishing wave vector in the barrier region and d is the width of each barrier (setting $q_0 d = 1$). Notice that the tunneling rate will be suppressed at a large k' .

Fig. 2 shows the calculated conductance of graphene quantum dot as a function of gate voltage at different temperatures, in which we take consideration of spin freedom. We find that the derived function of Fermi-Dirac distribution performs as a *Delta* function and it induces a conductance peak at position $E_N + U(N) - U(N - 1) = E_F$. The peak height maximum G_{max} , according to Eq. (5), is given by $G_{max} = \frac{e^2}{8k_B T} \Gamma$, which decreases linearly with increasing temperature in the quantum CB regime. Also, the N th peak probes the specific excitation spectrum around E_N , the quantum CB regime therefore usually shows randomly varying peak heights [7, 11, 12, 15]. We would also like to mention that in recent experiments [7, 8, 9] graphene dots have most likely rough edges which can induce electron scattering at the atomically sharp edges. Nevertheless we can find the lack of rough edges effect in the model described here does not change qualitatively the main features of the CB. Furthermore, the line shape of conductance can be obtained as

$$\frac{G}{G_{max}} = \cosh^{-2}\left(\frac{\delta}{2k_B T}\right), \quad \delta = E_N + U(N) - U(N - 1) - E_F, \quad (7)$$

which is consistent with the recent experimental observations in single electron transistor

on graphene nanoribbon [16].

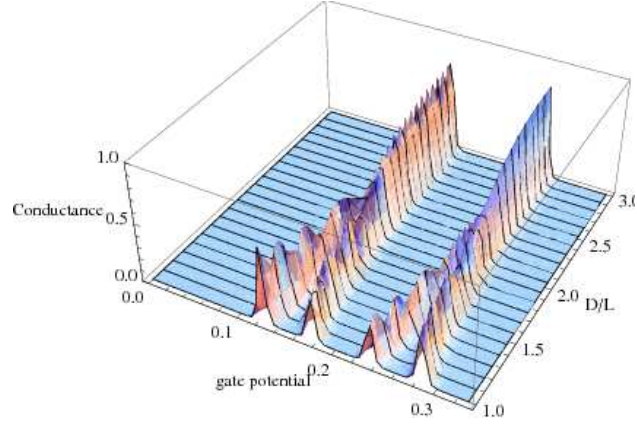
Graphene quantum dot array. In the following section, we investigate the conductance spectrum multiple coupled graphene quantum dot systems realized by assembling the above single dot separated from each other by a metallic gate. The type of coupling between quantum dots determines the character of the electronic states and the nature of transport through the quantum dot array. Here we use a Hubbard model to account for the effects of nearest interdot tunneling which is much smaller than the Coulomb energy of each dot, and neglect the long-ranged Coulomb interactions which are screened by the metallic gate [4].

We consider a doubly spin-degenerate state in each graphene quantum dot and to study the tunneling phenomenon in coupled dots. Due to the weak spin-orbit coupling in graphene, the spin degeneracy cannot be easily broken if without applying magnetic field. The tunneling strength in this case is determined by the interdot distance exponentially [4]. If the distance between the nearest dots is quite large compared with the dot size, the tunneling strength approaches zero, and the individual dot energy levels are conserved. As the interdot distance is decreased, the tunneling between nearest dots cannot be ignored, and the energy states are split into subbands, while spin degeneracy is still remained. As the discrete energy levels including the intradot Coulomb repulsion have been calculated above, it is convenient to get the tunneling coupled energy levels via direct diagonalization [18].

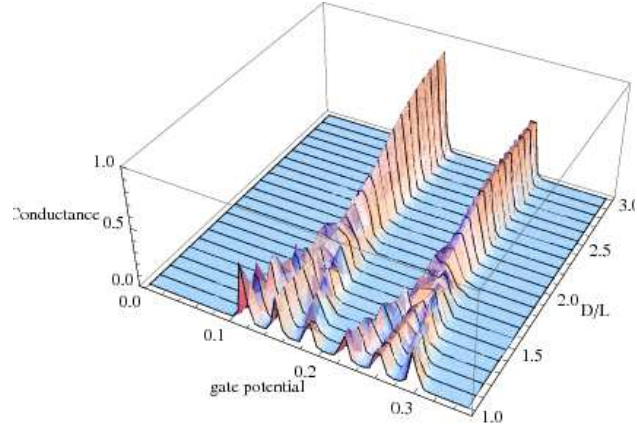
Fig. 3 shows the calculated conductance of two, three and four dots, from which, we find a remarkably phase transition for tunneling coupled graphene quantum dot array [17]. For weak interdot tunneling, i.e., when D/L is large (D is the distance between nearest dots and L is the length of a single dot), the Coulomb blockade of individual dots is maintained. The number of peaks is equal to the number of energy levels within a single graphene dot without interacting with surrounding dots. Each peak represents the addition of electrons to the array, one to each graphene dot at the same time. For the moment, transport through double graphene dots in this regime has been reported [10]. For intermediate D/L , the Coulomb blockade of individual dots is destroyed and a collective Coulomb blockade phenomenon appears. The original two energy states are split into two subbands and each capacitance peak is split into several peaks equal to the dot number. For stronger interdot tunneling strength, subbands will cross each other and the Coulomb blockade is destroyed altogether. All these theoretical predictions can be verified in the near future experiments.

Conclusion. In summary, we investigate the quantum dot behavior of electrostatically confined graphene nanoribbon. We study the single electron tunneling phenomenon at low temperatures of this system. The periodicity, amplitude and line shape of the CB oscillations are discussed in detail. Also, we have presented calculations of conductance spectra for multiple coupled graphene dots and find a phase transition from individual CB to collective CB as the coupling strength increases. The results presented here are important to provide necessary information for future experimental work.

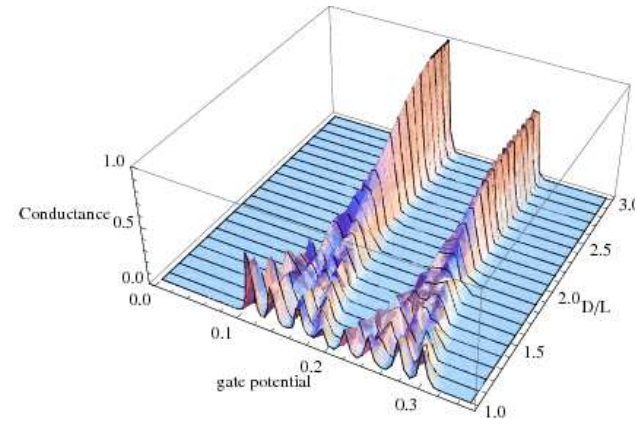
Acknowledgement. This work at USTC was funded by National Basic Research Programme of China (Grants No. 2006CB921900 and No. 2009CB929600), the Innovation funds from Chinese Academy of Sciences, and National Natural Science Foundation of China



(a)



(b)



(c)

FIG. 3: Plots showing the evolution of the Coulomb blockade oscillations as a function of the interdot tunneling strength D/L . D is the distance between two nearest graphene dots and L is the length of individual dot. Here we demonstrate the conductance spectrum of multiple coupled graphene dots for the case of (a) two, (b) three, (c) four. The gate voltage is in a unit of eV and the conductance is normalized by the highest peak.

(Grants No. 10604052 and No. 10874163 and No.10804104).

- [1] A. K. Geim and K. S. Novoselov, *Nature Materials* **6**, 183 (2008).
- [2] A. H. Castro Neto et al., *Rev. Mod. Phys.* **81**, 109 (2009).
- [3] P. G. Silvestrov and K. B. Efetov, *Phys. Rev. Lett.* **98**, 016802 (2007).
- [4] B. Trauzettel, D. Bulaev, D. Loss and G. Burkard, *Nature Physics* **3**, 192 (2007).
- [5] J. Milton Pereira, P. Vasilopoulos, and F. M. Peeters, *Nano Lett.* **7**, 946 (2007).
- [6] A. De Martino, L. Dell'Anna, and R. Egger, *Phys. Rev. Lett.* **98**, 066802 (2007).
- [7] L. Ponomarenko et al., *Science* **320**, 356 (2008).
- [8] C. Stampfer et al., *Appl. Phys. Lett.* **92**, 012102 (2008).
- [9] C. Stampfer et al., *Nano Lett.* **8**, 2378 (2008).
- [10] F. Molitor et al., arXiv:0905.0660.
- [11] J. H. Bardarson, M. Titov, and P. W. Brouwer, *Phys. Rev. Lett.* **102**, 226803 (2009).
- [12] J. Wurm et al., *Phys. Rev. Lett.* **102**, 056806 (2009).
- [13] C. W. J. Bennakker, *Phys. Rev. B* **44**, 1646 (1990).
- [14] H.-Y. Chen, V. Apalkov, and T. Chakraborty, *Phys. Rev. Lett.* **98**, 186803 (2007).
- [15] F. Libisch, C. Stampfer, and J. Burgdorfer, *Phys. Rev. B* **79**, 115423 (2009).
- [16] C. Stampfer et al., *Phys. Rev. Lett.* **102**, 056403 (2009).
- [17] C. A. Stafford and S. Das Sarma, *Phys. Rev. Lett.* **72**, 3590 (1994).
- [18] E. Dagotto et al., *Phys. Rev. Lett.* **67**, 1918 (1991).